

## Simulation of an Innovative Stand-Alone Solar Desalination System Using an Organic Rankine Cycle\*

Andreas Schuster\*\*, Jürgen Karl  
Technische Universität München, Institute of Energy Systems  
Boltzmannstr. 15, 85748 Garching, Germany  
E-mail: schuster@es.mw.tum.de, phone: +49-89-289 16269

Sotirios Karellas  
National Technical University of Athens, Laboratory of Steam Boilers and Thermal Plants  
9 Heroon Polytechniou, 15780 Athens, Greece

### Abstract

The rising of the world's population leads automatically to the rising of water demand. As a consequence the lack of drinking water increases. Since a large part of the world's population is concentrated in coastal areas, the desalination of seawater seems to be a promising solution. An innovative stand-alone solar desalination system could be used to produce drinking water from seawater. The great advantage of such a system is that it combines efficient desalination technology, reverse osmosis, with a renewable energy source, solar radiation. Thermal energy produced by the solar array evaporates a working fluid, which is used in an organic Rankine cycle that drives the pumps needed for the reverse osmosis process. Due to the fluctuation of solar irradiation, the dynamic simulation of such a system is necessary in order to assure the sufficient supply of water throughout a year. The simulation provides important information for optimum system sizing and design. The aim of this work is to present a modelling of a solar desalination system and to investigate the impact of different working fluids, thermodynamic parameters and cycle variations on the efficiency and water production of such a system.

*Keywords: Organic Rankine Cycle (ORC), desalination, reverse osmosis, solar radiation.*

### 1. Introduction

Between 1940 and 1990 the world's population reduplicated along with per capita water consumption. Over 436 million people live in countries with a lack of water. Due to the fact that more than 50 % of the world's population reside in coastal areas, desalination of seawater is an important option to overcome the insufficient water supply in these countries (Deutsche Meerwasser Entsalzung e.V., 2005).

The term "Seawater Desalination" comprises all the processes that remove dissolved salts from seawater with the aim of obtaining water with a low content of dissolved salts and impurities for use as drinking water for human needs, as process water for industry or as water for irrigation in agriculture.

Desalination processes can be divided in processes with and without phase change.

Processes with phase change are methods with evaporation like Multi-Stage-Flash-Evaporation (MFS) (Naffey et al., 2006), Multi-Effect-Distillation (MED) (Fiorini et al., 2007), Thermal or Mechanical Vapor Compression (TVC, MVC) (Mabrouk et al., 2007) and Solar Distillation (Alarcón-Padilla et al., 2007). Processes without phase change are represented by Reverse Osmosis (RO) and Electrodialysis (ED) (Hiersig, 1995).

Reverse Osmosis has the lowest consumption of energy per m<sup>3</sup> of desalinated water. Raulyu et al. (2006) mentions that the energy consumption of RO technology is 5-6 times lower than thermal

\* An initial version of this paper was published in October, 2005 in the proceedings of SIMS2005, Trondheim, Norway.

\*\* Author to whom correspondence should be addressed.

technologies. This consumption is mainly linked to the high pressure pump which feeds the reverse osmosis membrane with seawater. Solar energy can cover this energy need if it is converted into mechanical energy. A favorable process for this conversion could be a solar heated organic Rankine cycle.

There are several approaches for the application of solar / low temperature Rankine cycles for power or electricity production. Nguyen et al. developed a low temperature Rankine cycle system generating electricity with an efficiency of 4,3 % using n-Pentane as a working fluid (Nguyen et al., 2001). Riffat (2001) applied a solar / gas driven low temperature organic Rankine cycle for trigeneration. The efficiency of a water pumping system propelled by a solar Rankine cycle was analyzed by Aghamohammadi et al. (2001).

Although the system's components are well-known technologies, the integration to a fully and efficiently working system is a challenge. The components of the system have to be designed and tuned to each other in order to assure high efficiency and consequently high fresh water production rates. Instead of using energy storages, the produced fresh water will be stored. Special attention has to be paid on the part load behaviour of the system, according to intermittent solar irradiation.

The above makes it necessary to model the whole system and simulate it dynamically in order to quote the influences of different working fluids, variations of cycle design and thermodynamic parameters on the water production. Also a sufficient supply of fresh water throughout the whole year has to be validated. The simulation which is presented in this study is based on a European research project COOP-CT-2003-507997 called RO-Solar-Rankine, with the aim of constructing a desalination system using the above described technology.

## 2. Description of the System

The system layout is illustrated in *figure 1*.

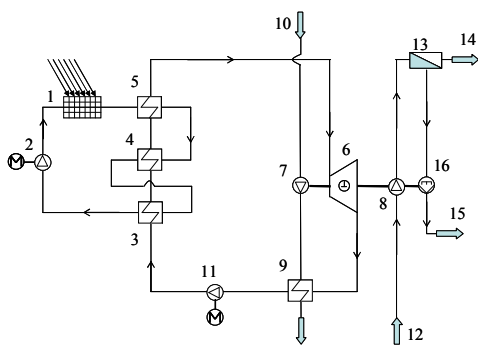


*Figure 1. Schematic representation of the system*

A field of evacuated tube collectors (1) with a size of 100 m<sup>2</sup> heats the collector fluid, circulated by a circulation pump (2). The collector fluid preheats (3), evaporates (4) and superheats (5) the organic working fluid. The superheated vapor is expanded in a scroll expander (6) generating mechanical work for the cooling water (7) and the seawater feed pump (8). The expanded vapor is condensed in a condenser (9), and cooled with seawater (10). After this, the feed pump (11) pumps back the working fluid.

The seawater feed pump (8) raises the pressure of the seawater (12) which will be desalinated. In the reverse-osmosis-membrane (13) the separation from clean water (14) and briny water (15) takes place. The clean water leaves the membrane and is drained to a storage tank. An energy recovery device (16) re-extracts the hydrostatic energy of the fluid; after this the brine is drained back to the sea.

## 3. Simulation Procedure

As mentioned above, dynamic simulation considering the changing of solar irradiation and temperature as well as part load behaviour has to be done. On this account the fast adjusting processes like the Reverse Osmosis Cycle and the Organic Rankine Cycle are modelled in the process simulation environment IPSEpro. IPSEpro is a high flexible software tool used for heat balance analysis of power plants, component design, acceptance test calculations and on-line optimization (SimTech Simulation Technology, 2007). The software contains libraries of standardized components, like turbines, heat exchangers, pumps etc. Each component is represented by a set of variables and equations. After building the model of the process in the flow sheet editor (see Screenshot in *Figure 2*) all the component equations are joined into a single system of equations. In a first analysis phase, this system is checked for errors. If the specifications are correct, the optimum solution method is determined. After this, the equations are solved with the numerical methods defined in the analysis phase.

IPSEpro provides different model libraries for various applications (e. g. in the field of power plants or desalination systems). If the predefined models are not sufficient, they can be modified with the Model Development Kit (MDK). MDK allows changing the component model equations and gives the possibility to the user to create his own models.

IPSEpro provides only steady state solutions. In order to obtain the dynamic system behaviour IPSEpro has to be linked to an external algorithm. Thus the transient processes, like the warm-up of

the collector field and the alteration of climate data are managed with Microsoft® Excel. Excel provides the input values for the IPSEpro calculation (e.g. collector temperature). After solving the system the values of interest are requested by a visual basic macro and saved in an Excel Sheet for later analysis.

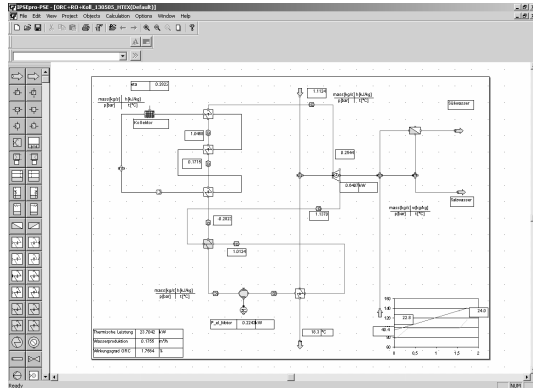


Figure 2. Screenshot of IPSEpro

## 4. Modelling of the Components

### 4.1. Collector loop

#### 4.1.1. Collector

The aim is to calculate the heat flow, which can be provided by the collector array. For the prototype plant evacuated tube collectors with direct flow will be used. The collector is modeled with the Equations (1) to (4).

$$\dot{q}_{coll} = \eta_0 \cdot (K_{\theta b} \cdot G_b + K_{\theta d} \cdot G_d) - k_1 \cdot \Delta T - k_2 \cdot \Delta T^2 - C_{eff} \cdot \frac{dT_{coll}}{dt} \quad (1)$$

$$\Delta T = T_{coll} - T_{amb} \quad (2)$$

The experimentally determined parameters of Equation (1) are all related to the aperture area of the collector. Therefore overall heat flow is calculated as product of specific heat flow and aperture area (see Equation (5)). The aperture area is defined as the maximum projected area through which unconcentrated solar radiation enters a collector (Norm DIN, 2001).

$$K_b(\theta) = \frac{\eta(\theta)}{\eta_0} = K_b(\theta_L) \cdot K_b(\theta_T) \quad (3)$$

$$K_d(\theta) = const \quad (4)$$

Due to the fact, that tilted irradiation causes lower absorption, the incidence angle modifiers (IAM) have to be considered. For optical asymmetric collectors like evacuated tube collectors, it is a product of the IAM for the

longitudinal and transversal incident angle (see Equation (3)). For diffuse irradiation which has no incidence angle the IAM has a constant value (see Equation (4)) (Isakson et al., 1993).

$$\dot{Q}_{coll} = \dot{q}_{coll} \cdot A_{aperture} \quad (5)$$

With the discrete form of the combination of equation (1) to (5) it is possible to calculate the collector temperature after a specific time step.

$$T_{coll,t} = \frac{\dot{Q}_{coll} \cdot \Delta t}{C_{eff} \cdot A_{aperture}} + T_{coll,t-\Delta t} \quad (6)$$

For the operation of the collector after the warm up matched flow and steady collector temperatures are assumed. The mass flow can be calculated with Equation (7).

$$\dot{m}_{coll} = \frac{\dot{Q}_{coll}}{c_p \cdot (T_{coll,in} - T_{coll,out})} \quad (7)$$

### 4.1.2. Climate data

In order to calculate the monthly mean daily water production rates for different sites, the climate data of the site is needed. Therefore climate data in hourly values for temperature, beam and direct irradiation is provided from Meteonorm, a state of the art global meteorological database (Meteonorm, 2005). It includes over 7,400 weather stations; an interpolation for other sites is included. It is important to have a climate dataset which not only complies with long-term yearly and monthly mean values, but also represents the maxima, minima and the characteristically devolution of the values of interest.

## 4.2. Organic Rankine cycle

### 4.2.1. Scroll expander

Commonly used turbines are available mostly in a power range above 50 kW. The aim was to find a market available power machine in a range of performance smaller than 10 kW. A very promising machine is the scroll expander, which is a modification of a climate compressor commonly used for car air conditioning. Scroll expanders are positive displacement machines consisting of two identical helical coils. One of these coils is fixed and the other coil is orbiting with 180° out of phase. So it forms crescent-shaped chambers, whose volumes accelerate with increasing angle of rotation.

Figure 3 illustrates the working principle of a scroll expander. High pressure vapor flows from the intake of the expander (1) towards the exhaust

(2). By orbiting the moving helical coil (3) forms closed chambers (4) with the fixed helical coil (5). The main steps are shown in part c): intake (6), expansion (7) and exhaust (8).

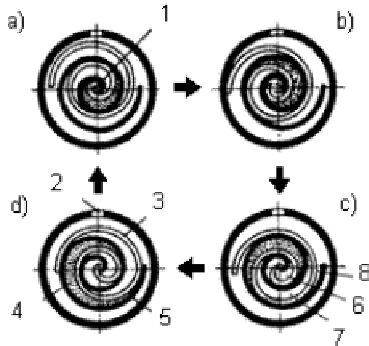


Figure 3. Scroll Expander (Schramek, 2001)  
a – b – c – d: sense of operation

The scroll expander is modeled as expansion machine (see Equation (8)) including part load behavior. Therefore the isentropic efficiency is calculated as a product of the isentropic efficiency in the design point and a mass depending function which indicates the efficiency's dependence on the live vapor mass flow.

$$P_{mech} = \eta_s \cdot \dot{m} \cdot (h_5 - h_4) \quad (8)$$

$$\eta_s = \eta_{s0} \cdot f\left(\frac{\dot{m}}{\dot{m}_0}\right) \quad (9)$$

#### 4.2.2. Working fluid

As the scroll expander is adapted from air-conditioning technology, working fluids were selected from a huge variety of refrigerants. For the selection different criteria have to be taken into consideration. The working fluid should offer a satisfying cycle efficiency with the given process parameters. But this is not the only criteria. The Montreal Protocol, an international treaty for the protection of the stratospheric ozone layer, and the EC regulation 2037/2000 restrict the use of ozone depleting substances (European Parliament, 2004). Although the use of the substances is not restricted, they should have low ozone depletion potential and low global warming potential. Further criteria are safety reasons like the maximum allowable concentration and the explosion limit, as well as technical requirements like boiling and condensation pressures.

### 4.3. Osmosis process

#### 4.3.1. Reverse osmosis membrane

Osmosis is the process of diffusion of a solvent through a semi permeable membrane whereas the solute diffuses to the side with the higher concentration of solute (see figure 4 a).

The diffusion of solvent continues till the osmotic pressure on both sides of the membrane is assimilated (see figure 4 b). Due to the water flow to the side with the formerly higher concentrated solution the liquid level and therefore the hydrostatic pressure (equal to the osmotic pressure) is higher. If pressure higher than the osmotic pressure difference on the side with the saline solution is applied, pure water is forced through the membrane (see figure 4 c).

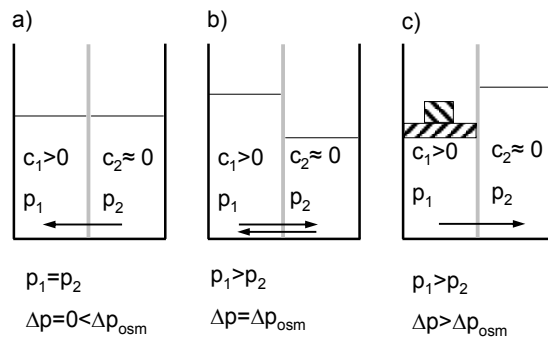


Figure 4. Membrane process (Hiersig, 1995)  
a) osmosis b) osmotic balance c) reverse osmosis

The osmotic pressure of a solution is calculated with Equation (10).

$$\Delta p_{osm} = \frac{1}{M_s \cdot v} \cdot (w_{rich} - w_{poor}) \cdot R \cdot T \cdot 10^{-2} \quad (10)$$

The model equations of a reverse osmosis membrane are as follows:

$$\dot{m}_p \cdot (1 - w_p) = \frac{A \cdot A^* \cdot (\Delta p_{mem} - \Delta p_{osm})}{v_p} \quad (11)$$

The permeate mass flow is calculated from Equation (11). Although the membrane is ideally permeable only for pure water, in reality small amounts of salt pass through the membrane. This dependency is described with Equation (12).

$$\dot{m}_p \cdot w_p = B^* \cdot A \cdot (w_{mem} - w_p) \quad (12)$$

At the surface of the membrane there is a higher concentration of solute because the pure water is forced through the membrane and the solutes are held back. The solutes diffuse away against the direction of feed water flow. The concentration at the membrane surface adjusting can be calculated with Equation (13) (Merlin et al., 2004).

$$w_{mem} = w_p + \left( \frac{w_F + w_R}{2} - w_p \right) \cdot e^{\left( \frac{\dot{m}_p \cdot v_p}{k_s \cdot A} \right)} \quad (13)$$

#### 4.3.2. Energy-recovery unit

Because of the relative low recovery by the desalination of seawater the use of energy recovery devices is very common. For this project it is foreseen to install an energy recovery unit. For large scale reverse osmosis plants pump / turbine combinations like turbochargers in cars are often used. Another possibility to recover energy in particular in small scale RO-plants is to use the so-called Clark pump.

Figure 5 illustrates the function principle of a Clark pump. The device consists of a movable piston (a) and a valve for changing the flow direction (not shown). The medium pressure from the feed pump and the pressure in the retentate are added to push the feed into the membrane (b) and to discharge the retentate in the neighbor chamber. After the valve changed the direction of the flow the process restarts. For the simulation the energy recovery device is considered as continuously moving part, the recovered energy is considered to be added to the shaft.

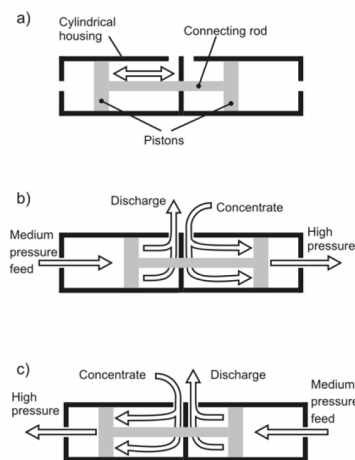


Figure 5. Clark Pump (Thomson et al., 2002)

## 5. Results

### 5.1. Refrigerants taken under consideration

As mentioned above a preselection concerning the working fluid was done. An overview over the selected fluids is given in TABLE I.

TABLE I. LIST OF FURTHER EVALUATED FLUIDS

Refrigerant	T <sub>c</sub> [°C]	p <sub>c</sub> [bar]	T <sub>s, 1 bar</sub> [°C]	p <sub>s, 20 °C</sub> [bar]
R134a	101.1	40.6	-27.1	5.7
R227ea	101.7	29.3	-16.5	3.9
R236fa	124.9	32.0	-1.4	2.3
R245fa	154.1	36.4	14.9	1.2

The fluids are given in the order of rising critical temperature T<sub>c</sub> and normal boiling temperature T<sub>s, 1 bar</sub>, whereas the critical pressure p<sub>c</sub> and the vapor pressure at 20 °C decline. This gives a first hint for the application of these working fluids. Fluids with higher critical temperature allow, on the one hand, higher boiling temperatures while on the other hand lower pressures and thereby lower pressure differences are reached.

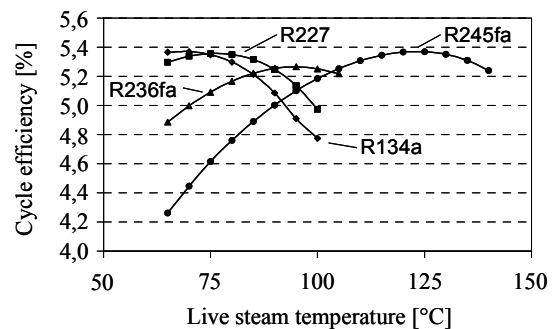


Figure 6. Cycle efficiency

In figure 6 the cycle efficiency is plotted over the live vapor temperature. A constant superheating of 5 K was assumed. Higher superheating to avoid liquid in the exhaust vapor is not necessary, because the expansion ends in the area of superheated vapor (see figure 7 and Figure 8). Higher superheating is favourable for higher efficiencies, but because of the low heat exchange coefficients this would lead to very large and expensive heat exchangers.

It is interesting, that the efficiencies are not monotonically increasing (see *figure 6*). The efficiencies have characteristic maxima. The reason for the decrease is the functioning principle of the scroll-expander. The scroll expander has a built-in pressure ratio called compression. The compression is a fixed value. If higher live vapor temperatures are applied (with fixed superheating), the vapor pressure rises. This leads to higher exhaust vapor pressures at the outlet of the expander to avoid deficient expansion. The fact, that the exhaust vapor pressure is equal to the condenser pressure leads to higher temperatures of heat removal, which is thermodynamically disadvantageous.

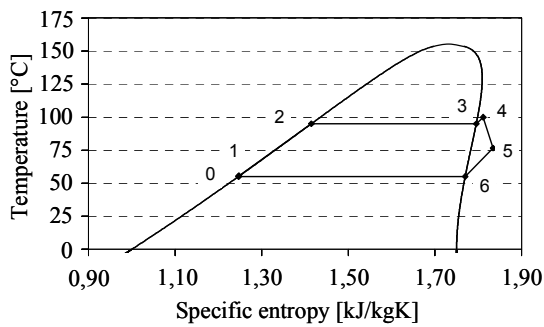


Figure 7. T-s Diagram 245fa  
0-1 compression in feed pump 1-2 preheating  
2-3 evaporation 3-4 superheating 4-5 expansion  
5-6 desuperheating 6-0 condensation

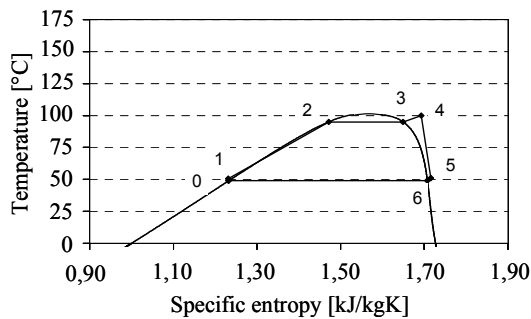


Figure 8. T-s Diagram R134a  
0-1 compression in feed pump 1-2 preheating  
2-3 evaporation 3-4 superheating 4-5 expansion  
5-6 desuperheating 6-0 condensation

## 5.2. Variation of the cycle

As mentioned above, the expansion of organic working fluids ends in the area of superheated vapor, as illustrated in *figure 7* and *figure 8*. Before condensing the exhaust vapor (from 6 to 0), it has to be desuperheated (from 5 to 6). A possible variation of the cycle is to integrate a heat exchanger (desuperheater) in order to preheat the condensate by desuperheating the exhaust vapor. This principle is shown in *figure 9*.

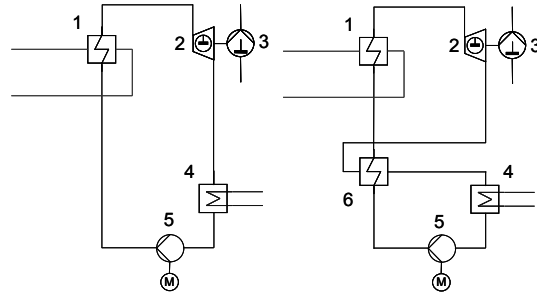


Figure 9. Organic Rankine Cycle with (left) and without desuperheater (right)  
1 heat exchanger, 2 scroll expander, 3 high pressure pump, 4 condenser, 5 feed pump, 6 desuperheater

The energy gained by desuperheating that can be used for preheating depends strongly on the fluid used in the cycle. Especially for fluids having a liquid saturation line with a positive slope, like R245fa (shown in *figure 7*) an increase of efficiency can be realised. If the fluid has a negative slope like R134a (shown in *Figure 8*), a desuperheater has no positive influence on the efficiency.

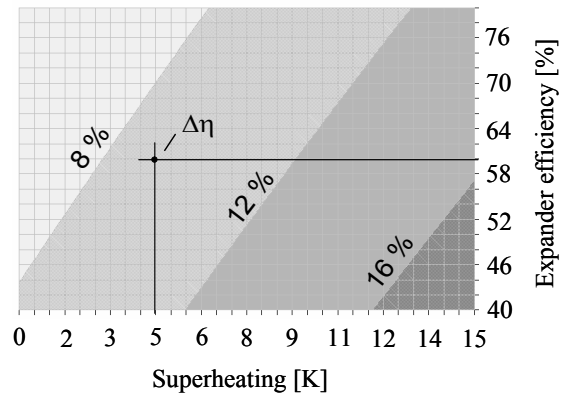


Figure 10. Influence of the desuperheater on the efficiency for R245fa

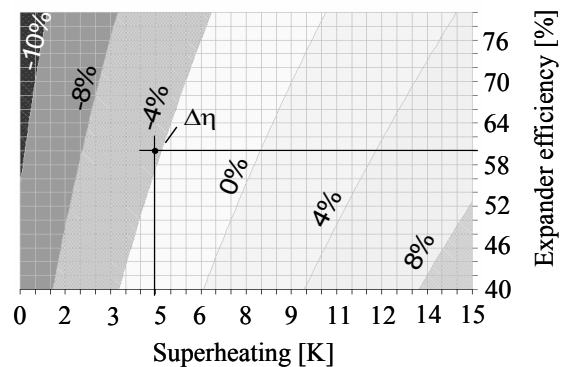


Figure 11. Influence of the desuperheater on the efficiency for R134a

Figure 10 and figure 11 show the influence of a desuperheater on the efficiency of the cycle. A reference case with a superheating of 5 K and an expander efficiency of 60 percent is marked. It can be seen, that with inclining superheating and declining expander efficiency the acceleration of the cycle efficiency increases. As mentioned above for R245fa a desuperheater improves the efficiency over a wide range, whereas for R134a, it has positive effects on the cycle only in the case of high superheating. This leads to additional cost, due to the need of large heat exchangers.

### 5.3. Dynamic calculations

The dynamic simulation allows a prediction of the distribution of the water production over a whole year. This allows the design of the desalination plant for specific requirements like high water production in summer time for hotels or more constant water production over the whole year for industries. It allows also an adequate dimensioning of water storage to assure the availability of water throughout the whole year. Transient effects are considered for the collector loop (like heating up and cooling down), the ORC and the RO-unit are calculated as steady-state.

An example for an achievable result is shown in figure 12. It shows the influence of different inclinations of the collector field on the mean daily water production for the reference site Athens. The optimum inclination for winter ( $\approx 61^\circ$ ) allows a more steady water production over the year than with an optimum inclination for summer ( $\approx 21^\circ$ ). On the other hand, the yearly water yield is  $876 \text{ m}^3$  (for  $61^\circ$ ) instead of  $1000 \text{ m}^3$  (for  $15^\circ$ ).

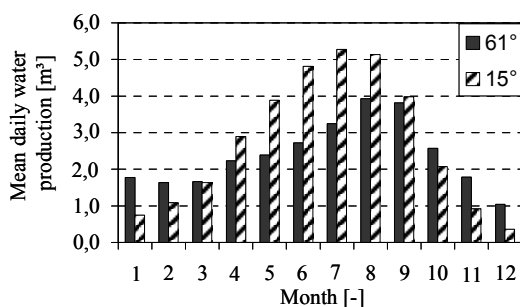


Figure 12. Influence of different inclination of the collector field on the mean daily water production

The simulation of a whole year in 15 minute steps needs approximately 2.5 h on an AMD Athlon XP 3000 with 2 GHz and 512 MB RAM.

### 5.4. Cost comparison

Besides the technical feasibility of the system, it is rather important to have a look on the achievable water production cost. In literature diverse comparisons of water production cost have

been made for large scale desalination plants (Reddy, 2007; Blank, 2007). The lowest cost can be reached with RO, Blank (2007) indicates freshwater cost of around  $1.10 \text{ \$/m}^3$  for a plant capacity of  $72,000 \text{ m}^3/\text{d}$  taking into account the current fuel prices. It is difficult to compare this presented stand-alone system with large centralized plants. For this purpose Manolakos et al. (2007) compared in the framework of this research project the water production cost of a PV-based RO-system with the ORC-based RO-system. The results are a water production cost of  $4.47 \text{ €/m}^3$  for the PV-RO-system and  $10.34 \text{ €/m}^3$  for the ORC-RO-system. The higher cost for the ORC-RO-system is caused by the higher installation cost (collector field). With a constant thermal source the water production cost declines to  $1.83 \text{ €/m}^3$ .

## 6. Conclusions

In this paper the dynamic simulation of a solar driven organic Rankine cycle powering a reverse osmosis desalination was presented. The division of the processes in transient and quasi steady state processes allows it to use a state of the art simulation environment for dynamic simulation. This has two advantages; it offers both short programming time and short computational time. The results of the simulation give hints for the choice of the working fluid as well as for the suiting live vapor parameters. Furthermore the simulation allows to optimize the cycle design concerning the working fluid.

To assure sufficient water production throughout the year, the mean daily water production gives a hint for the sizing of water storage systems. By varying the inclination of the collector surface the water production can be adjusted to the specific needs of the users.

## 7. Acknowledgements

The current work has been conducted within the framework of the European research project COOP-CT-2003-507997 "Development of an Autonomous Low-Temperature Solar Rankine Cycle System for Reverse Osmosis Desalination". The assistance of the European commission is acknowledged.

## Nomenclature

### Symbols

A	Area	$[\text{m}^2]$
A*	Membrane specific water permeability coefficient	$[\text{m/sbar}]$
B*	Membrane specific salt permeability coefficient	$[\text{m/s}]$
c	Concentration	$[\text{mol/l}]$
$c_p$	Specific heat capacity	$[\text{kJ/kgK}]$

$C_{\text{eff}}$	Effective heat capacity of collector	[kJ/m <sup>2</sup> K]
$G_b$	Beam irradiance in the plane of collector	[W/m <sup>2</sup> ]
$G_d$	Diffuse irradiance in the plane of collector	[W/m <sup>2</sup> ]
$k_1$	Collector loss coefficient	[W/m <sup>2</sup> K]
$k_2$	Collector loss coefficient	[W/m <sup>2</sup> K <sup>2</sup> ]
$k_s$	Salt mass transfer coefficient	[m/s]
$K$	Incident Angle Modifier	[-]
$M$	Molar mass	[kg/kmol]
$\dot{m}$	Mass flow	[kg/s]
$p$	Pressure	[bar]
$\dot{q}$	Area related heat flow	W/m <sup>2</sup>
$\dot{Q}$	Heat flow	[W]
$R$	General gas constant	[kJ/kgK]
$t$	Time	[s]
$T$	Temperature	[K]
$v$	Specific volume	[m <sup>3</sup> /kg]
$w$	Salt concentration	[kg/kg]
$\eta_0$	Zero loss collector efficiency	[-]
$\eta$	Efficiency	[-]

#### Subscripts

amb	Ambience
b	Beam
c	Critical
coll	Collector
d	Diffuse
F	Feed
L	longitudinal
mem	Membrane
osm	Osmotic
P	Permeate
R	Retentate
s	Saturation
S	Salt, Solute
T	Transversal
$\theta$	Incident angle

#### References

Aghamohammadi, M., Zarinchang, J., Yaghoubi, M., 2001, *Performance of a Solar Water Pump in Southern Iran*, Shiraz University, Shiraz, Iran.

Alarcón-Padilla, D.C., García-Rodríguez L., 2007, "Application of Absorption Heat Pumps to Multi-effect Distillation: C case Study of Solar Desalination", *Desalination*, 212, pp. 294-302.

Blank, J.E., Tusel, G.F., Nisan, S., 2007, "The Real Cost of Desalted Water and How to Reduce It Further", *Desalination*, 205, pp. 298-311.

Deutsche MeerwasserEntsalzung e.V., 2005, "Figures, Data and Facts to the Global Water Situation (Zahlen, Daten und Fakten zur weltweiten Wassersituation)", www.dme-

ev.de/global/downloads/Pressemeldungen/DME\_Fact\_Sheet\_Wasser.pdf (in German).

Duffie, J., Beckman, W., 1980, *Solar Engineering of Thermal Processes*, John Wiley & Sons, New York, Chichester, Brisbane, Toronto, Singapore.

European Parliament and council, 2004, *Regulation (EC) No 2037/2000 on Substances that Deplete the Ozone Layer*.

Fiorini, P., Sciubba, E., 2007, "Modular Simulation and Thermo-economic Analysis of a Multi-effect Distillation Desalination Plant" *Energy*, 32, pp. 459-466.

Hiersig, M. (editor), 1995, *Lexicon Manufacturing and Industrial Engineering (LexikonProduktionstechnik Verfahrenstechnik)*, VDI-Verlag GmbH, Düsseldorf. (in German).

Isakson, P., Eriksson, L., 1993, *MFC 1.0 $\beta$  Matched Flow Collector Model for Simulation and Testing*, Royal Institute of Technology, Stockholm.

Lemmon, E., McLinden, M., Huber, M., 2002, *NIST Reference Fluid Thermodynamic and Transport Properties – REFPROP*, U.S. Department of Commerce, National Institute for Standards and Technology, Gaithersburg, Maryland, USA.

Mabrouk, A.A., Nafey, A.S., Fath, H.E.S., 2007, "Thermo-economic Analysis of Some Existing Desalination Processes" *Desalination*, 205, pp. 354-373.

Manolakos, D., Mohammed, E.Sh., Karagiannis, I., Papdakis, G., 2007, "Technical and Economic Comparison Between PV-RO System and RO-Solar Rankine System. Case Study: Thirasia Island", *Conference on Desalination and the Environment*, Halkidiki, Greece, April 22-27, 2007.

Melin, Th., Rautenbach, R., 2004, *Membrane Operation (Membranverfahren)*, Springer Verlag, Berlin, Heidelberg, New York, (in German).

Meteonorm, 2005, *Global Meteorological Database for Engineers, Planners and Education*, Version 5.1, Edition 2005, Meteotest, Bern.

Nafey, A.S., Fath, H.E.S., Marbrouk, A.A., 2006, "Thermo-Economic Investigation of Multi Effect Evaporation (MEE) and Hybrid Multi Effect Evaporation- Multi Stage Flash (MEE-MSF) Systems" *Desalination*, 201, pp. 241-251.

Nguyen, V.M., Doherty, P.S., Riffat, S.B., 2001, "Development of a Prototype Low-Temperature Rankine Cycle Electricity Generation System". *Applied Thermal Engineering*, 21, pp. 169-181.

Norm DIN EN ISO 9488 March 2001, *Solar Energy Vocabulary*, Trilingual Version.

Raluy G., Serra L., Uche J., 2006, "Life Cycle Assessment of MSF, MED and RO Desalination Technologies". *Energy*, 31, pp. 2361-2372.

Reddy, K.V., Ghaffour, N., 2007, "Overview of the Cost of Desalinated Water and Costing Methodologies". *Desalination*, 205, pp. 340-353.

Riffat, S.B., Hicks, W., Nguyen, M., Doherty, P., 2001, *The Development and Testing of a Microtrigeneration System Driven by Solar/Gas*, Institute of Building Technology, University of Nottingham, Nottingham, UK.

Schramek, E.-R. (editor), 2001, *Pocket Book for Heating and Air Conditioning (Taschenbuch für Heizung und Klimatechnik)*, Oldenburg Industrier Verlag, München (in German).

SimTech Simulation Technologies, 2007, <http://www.simtechnology.com>, Company web page, (Date of access 03.07.2007).

Thomson, M., Miranda, M., Infield, D., 2002, *A Small-Scale Seawater Reverse-Osmosis System with Excellent Energy Efficiency Over a Wide Operating Range*, CREST, Loughborough University of Technology, UK.